Korean J. Chem. Eng., **25**(5), 1094-1102 (2008)

A CFD model for predicting the flow patterns of viscous fluids in a bioreactor under various operating conditions

Byung-Hwan Um*,† and Thomas R. Hanley**

*Forest Bioproducts Research Initiative, Department of Chemical and Biological Engineering, University of Maine, Orono, Maine 04469, USA
**Department of Chemical Engineering, Samuel Ginn College of Engineering, Auburn University, Auburn, Alabama 36849, USA
(*Received 11 December 2007 • accepted 7 March 2008*)

Abstract−Computational fluid dynamics simulation is becoming an increasingly useful tool in the analysis and design of simultaneous saccharification fermentation (SSF) and saccharification followed by fermentation process (SFF). To understand and improve mixing and mass transfer in a highly viscous non-Newtonian system, it was necessary to simulate the flow behavior in this bench scale bioreactor (BioFlo 3000). This study focused on designing a high concentration medium agitation system for such a process using the commercial computational fluid dynamics package Fluent (V. 6.2.20) and its preprocessor Mixsim (V. 2.1.10). The objective of this study is to compare performance of various designs of a bioreactor and identify the flow pattern and related phenomena in the bench scale tank. The configuration of the physical model for simulating a mixing tank with a Rushton impeller consists of an ellipsoidal cylindrical tank with four equally spaced wall mounted baffles extending the vessel bottom to the free surface, stirred by a centrally located six-blade Rushton turbine impeller. Simulations were performed with the original and a modified design in which the lower bottom shaft mounted a Lightnin A200 impeller. The results suggest that there is a potential for slow or stagnant flow between top impellers and bottom of the tank region, which could result in poor nitrogen and heat transfer for highly viscous fermentations. The results also show that the axial velocity was significantly improved for the modified geometry in the bottom of the tank.

Key words: Computational Fluid Dynamics (CFD), non-Newtonian Fluid, Saccharification Followed by Fermentation (SFF), Multiple Reference Frame (MRF) Model, High Solid Fermentation, Rushton Turbine, k-ε Turbulence Model

INTRODUCTION

The process of designing, building and evaluating bioreactors for high-substrate concentration fermentation is both costly and time consuming [1,2]. The use of a computational fluid dynamics (CFD) model can aid in bioreactor development by providing detailed information on the hydrodynamic and chemical environments necessary for optimal hydrolysis and cell growth.

To obtain the 5 per cent (v/v) ethanol production needed for an economically viable industrial-scale ethanol distillation, a high glucose concentration is also needed. This can only be achieved when a high initial cellulose concentration is combined with a favorable conversion yield of cellulose into soluble sugars. Using high substrate concentration in the form of fibrous, solid materials poses a problem: high viscosity prevents efficient mixing. It has been reported repeatedly that solid concentrations above 10 per cent resulted in poor ethanol yield due to inefficient mass transfer [3,5].

Agitation in bioreactors is an important process design factor that can influence the hydrolysis operation in several ways. Considering the heterogeneity of the hydrolysis reaction environment, in which a liquid enzyme acts on a solid substrate, adequate mixing is required to ensure sufficient contact between the reactants, as well as to promote heat and mass transfer within the reaction vessel. Moreover, it has been shown that excessive mixing can deactivate the enzyme and microorganism reducing production (sugar/ethanol) yields, owing to the shear force generated by the mixer and the entrapment of air bubbles into the medium at the air liquid surface [6,7]. Therefore, one way of improving the problems of the overall process is to determine the optimum level of mixing, reducing the extent of shear-induced enzyme and microorganism deactivation and lowering the mixing energy costs.

For this study, the FLUENT 6.2 commercial computational fluid dynamics package was used to predict the flow-pattern and transport phenomena in the 3 L bioreactor, to aid in the design of a high solid fermentation and to provide methodologically a loading method of substrate for the high viscous SFF process in large-scale. Simulation was performed by using the original bioreactor produced by New Brunswick Scientific and the modified design in which the lower bottom shaft mounted Lightnin A 200 was added.

MATERIALS AND METHODS

1. Vessel Geometry

The configuration of the physical model for simulating a mixing tank with Rushton impeller consists of an ellipsoidal cylindrical tank with four equally spaced wall mounted baffles extending from the vessel bottom to the free surface, with stirring by a centrally located six-blade Rushton turbine impeller. The tank diameter measures 0.138 meter, and baffle width is 0.008 meter. The impeller diame-

†To whom correspondence should be addressed.
E-mail: BHUm@umche.maine.edu

ter was 0.046 meter (D/T=3) for all impellers. The impellers were mounted on a 0.0025 meter diameter shaft rotating at 120 and 240 RPM. The distance between the impellers was 0.061 meter. The impeller center was positioned at a distance C=T/3 off the tank bottom. The liquid level was equal to the tank diameter, Z/T=1.3.

2. Convergence Criteria and Blend Time

Simulations were typically considered converged when the scaled residuals (continuity, X, Y, Z-velocity, k, and ε), normalized relative to the maximum circulating flow, fell below 6E-04 by iteration 5,000. Further checks for convergence were made by verifying that global quantities, such as the power number, and the circulation number, were constant.

The model predictions are compared with the results of the experimental blend time correlation. Mixsim can compute the blend time for a single impeller in a tank, as well as the effective blend time for a tank with multiple impellers.

The blend time to achieve 99 per cent uniformity in a tank with a multiple impellers is computed from [8].

$$t_{99}=\frac{4.605}{k_{m,eff}}$$

where a sum over all impellers (i=1 to n) is performed to computer $k_{m,eff}$:

$$k_{m,eff}=\sum_{i=1}^{n}k_{m,i}=\sum a_i N_i\left(\frac{D_i}{T}\right)^{b_i}\left(\frac{T}{Z}\right)^{0.5}$$

All of the graphs show uniformity above 99% at t=13.37 s. And, all calculations were steady state.

3. The k-ε Mathematical Models

The basic two transport equations that need to be solved for this model are for the kinetic energy turbulence, k, and the rate of dissipation of turbulence, ε [9]:

$$\frac{\partial(\rho k)}{\partial t}+\frac{\partial}{\partial x_i}(\rho U_i k)=\frac{\partial}{\partial x_i}\left(\mu+\frac{\mu_t}{\sigma_k}\right)\frac{\partial k}{\partial x_i}+G_k-\rho\varepsilon \qquad \text{Transport Eq. (1)}$$

$$\frac{\partial(\rho\varepsilon)}{\partial t}+\frac{\partial}{\partial x_i}(\rho U_i \varepsilon)=\frac{\partial}{\partial x_i}\left(\mu+\frac{\mu_t}{\sigma_\varepsilon}\right)\frac{\partial \varepsilon}{\partial x_i}+C_1\frac{\varepsilon}{k}G_k+C_2\rho\frac{\varepsilon^2}{k} \qquad \text{Transport Eq. (2)}$$

The quantities C_1, C_2, σ_k, and σ_ε are empirical constants. The quantity G_k appearing in both equations is a generation term for turbulence. It contains products of velocity gradients, and also depends on the turbulent viscosity:

$$G_k=\mu_t\left(\frac{\partial U_i}{\partial x_j}+\frac{\partial U_j}{\partial x_i}\right)\frac{\partial U_j}{\partial x_i} \qquad \text{Turbulence energy Eq. (3)}$$

Other source terms can be added to Eqs. (1) and (2) to include other physical effects such as swirl, buoyancy or compressibility, for example. The reference values of the model constants were the consensus ones C_μ=0.09, C_1=1.44, C_2=1.92, σ_k=1.0, and σ_ε=1.3.

$$\mu_t=\rho C\mu\frac{k^2}{\varepsilon} \qquad \text{Eddy viscosity (4)}$$

To summarize the solution process for the k-ε model, transport equations are solved for the turbulent kinetic energy and dissipation rate. The solutions for k and ε are used to compute the turbulent viscosity, μ_t. The above governing equations are solved by using the finite volume method implemented in CFD code-FLUENT 3-D; steady-state simulations are carried out by using the segregated solver with absolute velocity formulation.

4. Constant N_p and P per Liquid Volume

$$P=a\left(\frac{H_b}{0.2D}\right)\left(\frac{N_b}{6}\right)^b \qquad (5)$$

$$N_{Re}=\frac{D^2N\rho}{\mu} \qquad (6)$$

$$N_p=\frac{P}{N^3D^5\rho} \qquad (7)$$

N_{Re} : Reynolds number
a, b : constant value (radical disk impeller, a=5, b=0.8)
N_p : power number, ratio of applied force to mass times acceleration
P : power input [W]
ρ : density of liquid [Kg/m^3]
N : impeller speed [rpm]
N_b : impeller blade number
H_b : disk height [m]
D : impeller outer diameter [m]

5. Simulation Model and Tool Package

- Type: 3D cylindrical
- Analysis model: Multiple Reference Frame (MRF)
- Turbulent model: Standard k-ε model
- Mixsim V. 2.1.10
- FLUENT V. 6.2.20

6. Bioreactor Operating Conditions

To maximize the glucose and ethanol concentrations, substrate concentrations were employed from 10 to 20 per cent on a dry basis, corresponding to cellulose concentrations of 8 to 17 per cent. In several studies for traditional batch enzyme reaction and fermentation of high substrate concentration (>10 per cent), there was no visible liquid phase due to complete absorption of liquid by the biomass. To overcome this problem the Solka Floc was added to the reac-

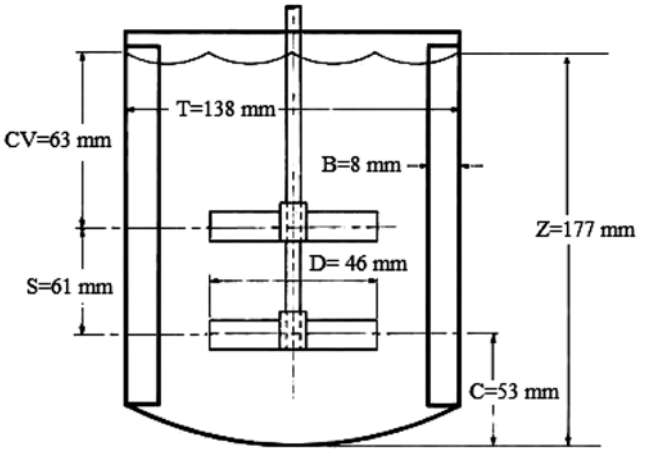

Fig. 1. Nomenclature used to describe the mixing system: T=Vessel diameter, Z=Liquid fill level, D=Impeller diameter, B=Baffle width, C=Impeller clearance, CV=Coverage, S=Spacing between impellers.

tions in three portions during both enzyme reaction and fermentation up to the 20 per cent final substrate concentration. The portions were added to the reaction in the initial four hours of the reaction. Then, the inoculum prepared as 10 per cent by volume of the total working volume (2 L) was transferred into the reactor after enzymatic hydrolysis for 48 hours. The enzyme loading was 20 FPU per gram of cellulose, supplemented by β-glucosidase to prevent product inhibition by cellobiose. The SFF experiments were operated for 96 hours, initially at 50 °C and finally at 30 °C. The viscose fermentation broth used in these projects exhibited pseudoplastic rheology that is modeled quite well over a wide range of shear rates by the Herschel-Bulkley model. Consequently, the Herschel-Bulkley was used to model fluid rheology in this study, with 0.233, 1.430, and 3.020 Pascal-second for 10, 15, and 20 per cent concentration at average impeller shear rate in the reactor, respectively. And, the average particle size was 44.0, 53.0, 57.5 μm for the SFF process at 10, 15, 20 percent initial solids, respectively.

RESULTS AND DISCUSSION

1. Grid Refinement and Generation

The geometry was defined in the Cartesian (x, y, z) coordinate system. After the grid was generated, the skewness of 97.41 percent cells was below 0.6. It is very important to assess the quality of the grid, because properties such as skewness can greatly affect the accuracy and robustness of the CFD solution. In general, high-quality meshes contain elements that possess average Q values of 0.4. Even a single cell with skewness >0.98 may destroy convergence in the whole computation.

The computational grid was defined by 570,000 unstructured, nonuniformly distributed, 182,000 nodes, and tetrahedral cells. When refining the mesh, care was taken to put most additional mesh points in the regions of high gradient around the blades and discharge region.

The commercial mesh generator Mixsim 2.1.10 was used to create a structured, non-uniform multi-block grid, as shown in Fig. 2, with inner and outer zones by an interface in order to enable the use of multiple reference frame techniques. The wide nature of the impeller blades relative to the diameter of the hub results in the overlapping of blades close to the hub. Consequently, simulation of only part of the vessel in order to decrease computational expense was not possible, and therefore it was necessary to model the entire vessel geometry.

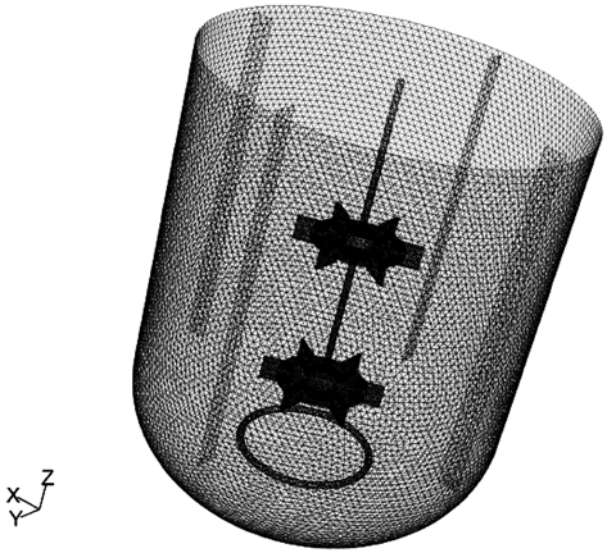

Fig. 2. Grid of working volume 2 L bench scale bioreactor.

Table 1. Reynolds number and power draw for suspension simulation as function of solid concentration at various RPM

Solid concentration [%, w/v]	Reynolds number [$Re=\rho ND^2/\mu$]	Power draw (W) [$P=N_p\rho N^3D^5$]
At 120 RPM		
0	4203.3	0.0082
10	248.6	0.0093
15	64.5	0.0097
20	50.3	0.0103
At 240 RPM		
0	8406.7	0.0655
10	497.1	0.0741
15	129	0.078
20	100.6	0.082

Note: SFF condition: 0-20% (w/v) solid concentration, 20 FPU/g of glucan, pH 4.8 to 5.0, 120 and 200 rpm, *Zymomonas mobilis*, strain 39679:pZB4L.

2. Turbulence in a Tank with Baffled Rushton Impeller

The blade predicted tip velocity V_{tip} at the rotational speed of 120 RPM was 0.29 m/s (Fig. 4), and an impeller Reynolds number and power draw based on tip speed and impeller diameter are summarized in Table 1. The resulting simulation of high solid suspension was in the laminar flow regime ($Re=\rho ND^2/\mu$, ranging from Re= 50 to Re=500). As the impeller Reynolds number decreased, a transition to radial flow occurred. At impeller Reynolds numbers less than 100, strictly radial flow is observed.

The standard k-ε turbulent model was employed to treat the strong swirling flow induced by Rushton impeller. Fig. 3 shows the predicted flow pattern for original and modified geometry in the mixing tank with Rushton turbine impeller. The maximum and minimum velocity magnitudes were slightly different at the bottom area of the tank. This slight difference may be caused by the lower bottom shaft mounted Lightnin A200 impeller.

3. Predicted Velocity Distribution

Fig. 3 shows the three types of steady-state flow patterns observed with the MRF models at the vertical baffle plane (tank-cut-plane 90°) at 15 per cent solids concentration. The magnitude of the velocity at any point in the flow field is indicated by the length and color of the arrow at that point.

A general pattern can be described as follows: a strong flow is found right at the two impellers pushing the fluid downward at an angle of about 45° for all of the concentrated suspensions. An upward flow can be found below the two impellers, along the tank wall between the two impellers, and right off of the tip of the impellers that in turn causes some circulation. Other circulation areas can be seen around the bottom of the tank. Some of the upward flow caused by the lower impeller is drawn back to the lower impeller,

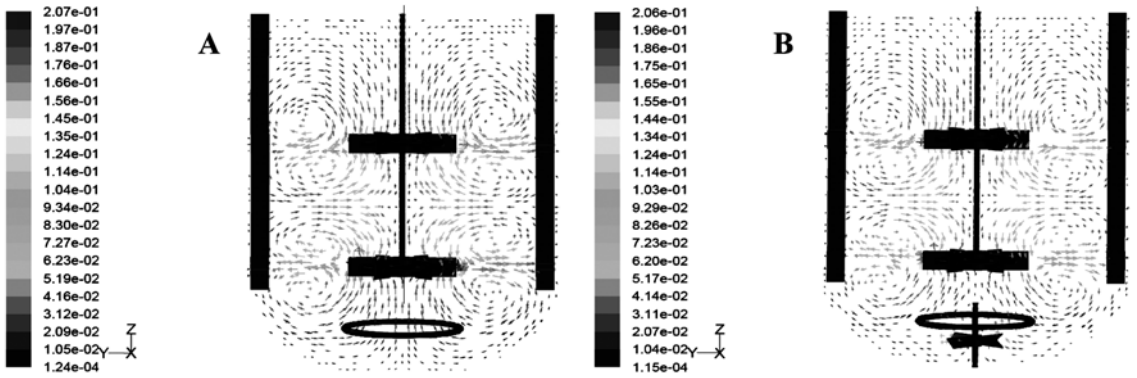

Fig. 3. Velocity vectors colored by velocity magnitude (m/s): original geometry (3A), modified geometyr (3B). Note: SFF condition: 15% solid concentration, 20 FPU/g of glucan, pH 4.8 to 5.0, 120 rpm, *Zymomonas mobilis*, strain 39679 : pZB4L.

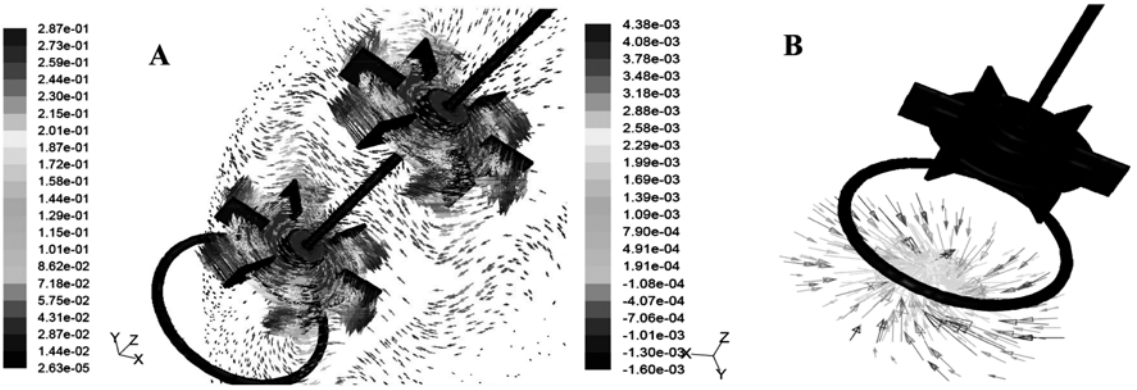

Fig. 4. Flow around impeller blade (4A) and axial velocity vectors on the bottom of tank (4B) colored by velocity magnitude (m/s). Note: SFF condition: 15% solid concentration, 20 FPU/g of glucan, pH 4.8 to 5.0, 120 rpm, *Zymomonas mobilis*, strain 39679 : pZB4L.

while some follows the center path upward to the upper impeller. Some of the flow pumped down by the upper impellers is drawn even further down by the lower impeller, with some other circulating back to the top. Little flow occurs in the region the fermentor wall. This primary circulation pattern is completed as the liquid reenters the impeller region at the top impeller. As a result of this flow pattern, there is virtually no movement of fluid between the gas-liquid interface and the top impeller.

The three plots generally show similar flow patterns with a strong primary circulation loop in the lower half of the tank and a smaller secondary loop below the impeller. Here in the discharge jet, there are not great differences in the predicted solution between the original and modified geometries around the impellers. This explains how the portion loading of substrates could reduce viscosity for the high solid fermentation compared to traditional high substrate loading.

4. Axial Velocity

The off-bottom particle suspension ability is critical to high solid ethanol fermentation. The axial velocity along the bottom is a key factor affecting the bioreactor off-bottom ability. Fig. 4B shows axial velocity vectors at the tank bottom. Higher upward axial velocity along bottom means higher off-bottom ability. It can be seen that axial velocity was rather small for relatively higher solid concentration at the bottom of the tank. Low axial velocity, color grade light grey (in case of black and white pictures), results in the solid suspension staying on the bottom of tank (Fig. 4B).

The contour of the axial velocity profile between tank bottom and fermentor wall is highly dependent on the value of the flow behavior index (n). As expected, higher values of n (n=1.55) produce a more parabolic profile, whereas low n values (n=0.74) produce a more blunt profile. Fig. 5 represents axial velocity contour plots, showing the effects of impeller speed on average velocity (m/s) in this region for original and modified geometries. From the contour plots, it is evident that the maximum values of V_{tip} ($0.096V_{tip}$ for 200 rpm, $0.047V_{tip}$ for 120 rpm (modified geometry), and $0.046V_{tip}$ for 120 rpm) are found below the agitator. The maximum V_{tip} increases as n increases.

To improve the off-bottom behavior, the axial velocities along the bottom in the three different operation conditions have been compared. For most of the conditions tested in this study, the circumferential averaging axial velocity is plotted for the different solid concentration as a function of tank radial position at the middle and bottom panel of the mixing tank in Figs. 6 and 7. The average velocities computed in the study varied from 0 to 0.003 m/s. As shown in Fig. 6, the axial velocity was significantly increased as rotational speed increased over all of the concentrations at the middle of tank. Fig. 7 shows the circumferential average axial velocity and comparison for various operation conditions at Z/T=0.04. The modified geometry resulted in a higher upward axial velocity than the original design for the 15 and 20 per cent concentration at the tank

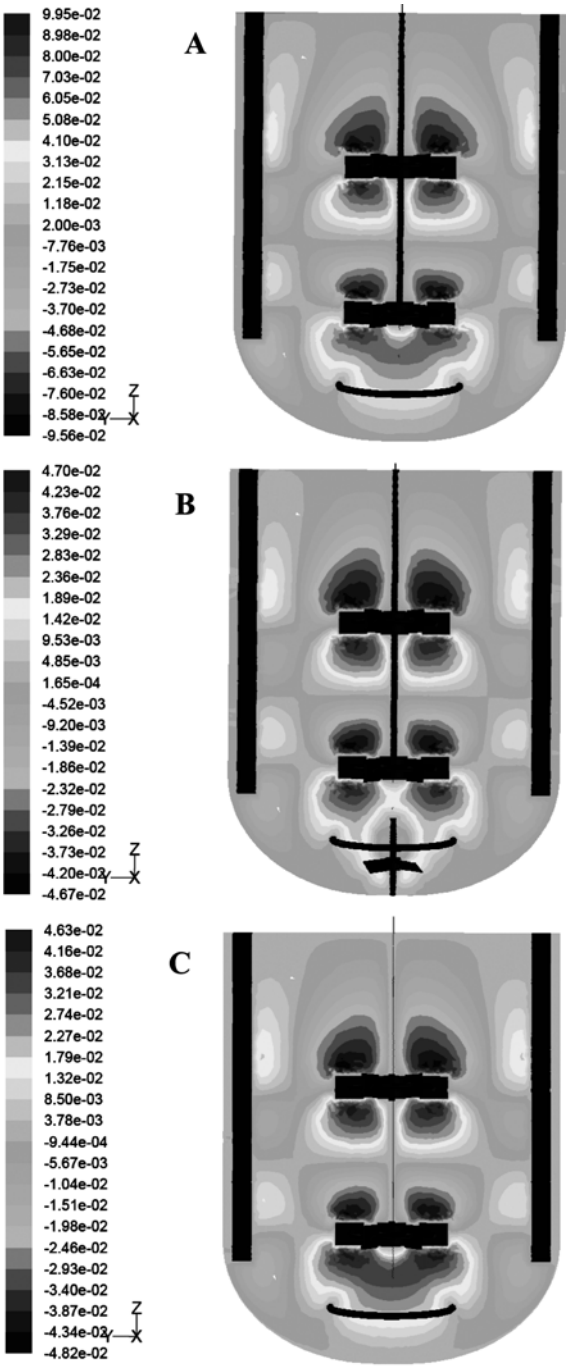

Fig. 5. Distribution of axial velocity (m/s) of working volume 2 L in a bench scale bioreactor. (5A): 200 rpm, (5B): 120 rpm (modified geometry), and (5C): 120 rpm. Note: SFF condition: 15% solid concentration, 20 FPU/g of glucan, pH 4.8 to 5.0, *Zymomonas mobilis*, strain 39679:pZB4L.

bottom. Figs. 7B and 7 C show that increasing RPM has no effect on solids flowing at the tank bottom (Fig. 7B, 7C).

On the other hand, a relatively weak upward flow was found near the center bottom of the tank and below the baffle, creating the circulation region (Fig. 5). Specifically, the reverse swirling suspension has been measured in a small region in the top of the upper impeller and in the corner of baffles with a minimal velocity (−0.096 V_{tip}, −0.047 V_{tip}, and −0.048 V_{tip}). These results imply that near the center bottom of the tank, the fluid axial velocities of the fluid were not uniform, perhaps resulting in the solid suspension staying on the bottom of tank. These phenomena were more significant as the solid concentration increased.

5. Stagnant and Slow Flow Zones

From the contour plots, conditions promoting essentially stagnant flow can be identified when the average velocity is on or below the 0 m/s contour color. Of course, if the anaerobic fermentation broth between the corner of baffles and the outer wall was completely stagnant, the cells would quickly become starved of nitrogen, nutrient, and stop synthesizing product. The model indicates that flow up the under baffle region can be stagnant at the impeller speed of 120 rpm and the distance between tank bottom and the baffles is 0.05 m.

In summary, it seems that, in addition to there being a potential for nitrogen nutrition starvation in the upper portion of the baffle-wall region when flow through this region is slow, there is also a potential for stagnant flow and nitrogen and nutrition starvation in the region between the top impeller and the gas-liquid interface when flow through the fermentor wall region is slow. In real fermentations, there is some surface aeration near the gas-liquid interface. As expected, the simulations with higher values of n exhibited larger low flow space.

6. Shear Stress and Turbulent Viscosity

An understanding of the velocity flow fields is a prerequisite to understanding mixing and key physical parameters such as shear stress, flow fluctuations, and vorticity fields. The circumferential averaging shear stresses are plotted for the different operating reactor conditions as a function of tank radial position on two different panels by z direction of the mixing tanking in Figs. 10 and 11. The fluid suspension near the blade wall is accelerated by an imbalance of shear forces. The average maximum values determined by circumferential averaging model on the middle of tank were near the impellers. The highest shear stress occurred in the tip of impeller at 240 RPM over all of the concentration (Fig. 10).

Fig. 8 shows the contour of the distribution of the turbulent viscosity, modeled by three different conditions. The maximum viscosity was found at the midpoint (z=0.09 m) of the tank 0.16 paschal-seconds for 240 RPM, 0.051 paschal-seconds for 120 RPM (modified geometry), 0.049 paschal-seconds for 120 RPM (original geometry) at 15 per cent solid concentration. It could be found that the turbulent viscosity distribution between the original and the modified geometry is not much different (Fig. 8B, 8C). With higher values of n, the fluid viscosity was less affected by shear and the fluid encountered a resistance that significantly impeded flow in the wall region.

Results for average shear stress and contour distributions of viscosity over the range of tank radial position in the mixing tank illustrated that the fluid viscosity was significantly reduced in the high shear stress regions. Consequently, the fluid encountered little resistance as it moved rapidly through this region.

7. Turbulence Dissipation Rate in Mixing Tank

The distribution of turbulent dissipation rates as shown in Fig. 9 is characteristic of the reactor geometry. Specifically, these turbulent dissipation rates have been used to obtain the local shear rates for calculating the fermentation broth viscosity. The turbulent ε was

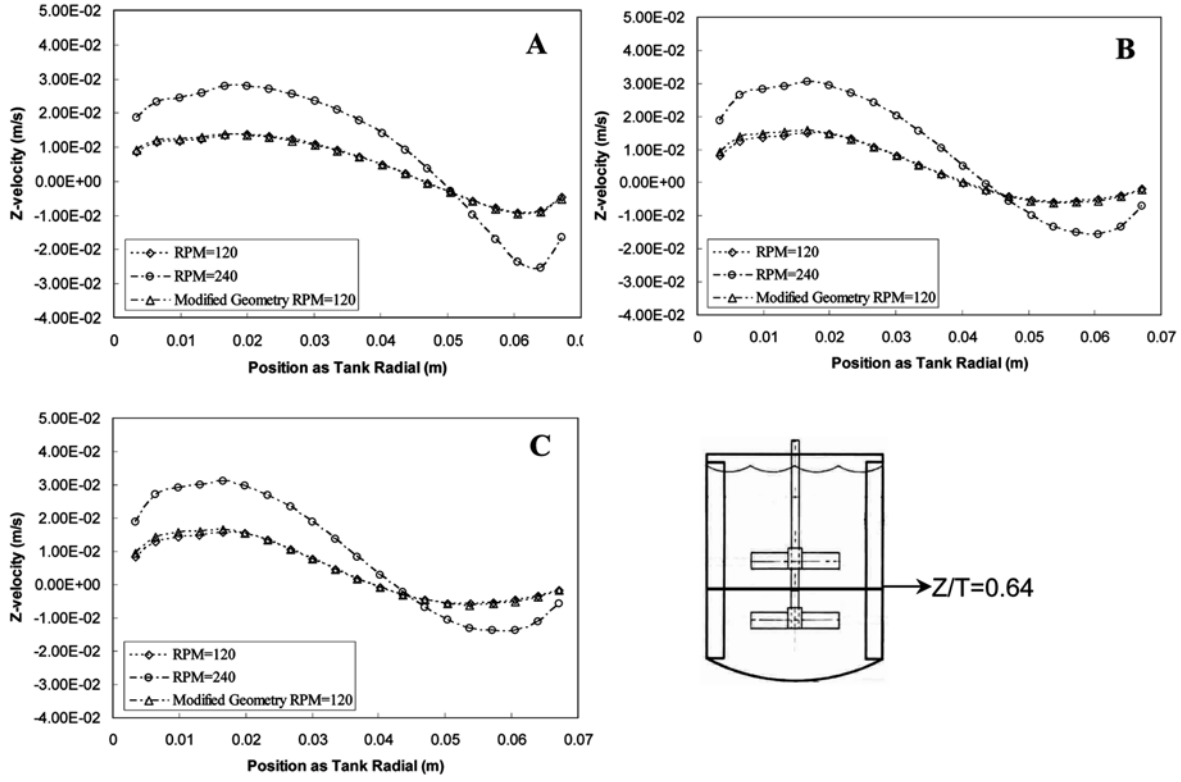

Fig. 6. Profiles of circumferential average axial velocity (m/s) of working volume 2 L bench scale bioreactor at Z/T=0.64. (6A): 10%, (6B): 15%, and (6C): 20% solid concentration. Note: SFF condition: 20 FPU/g of glucan, pH 4.8 to 5.0, *Zymomonas mobilis*, strain 39679 : pZB4L.

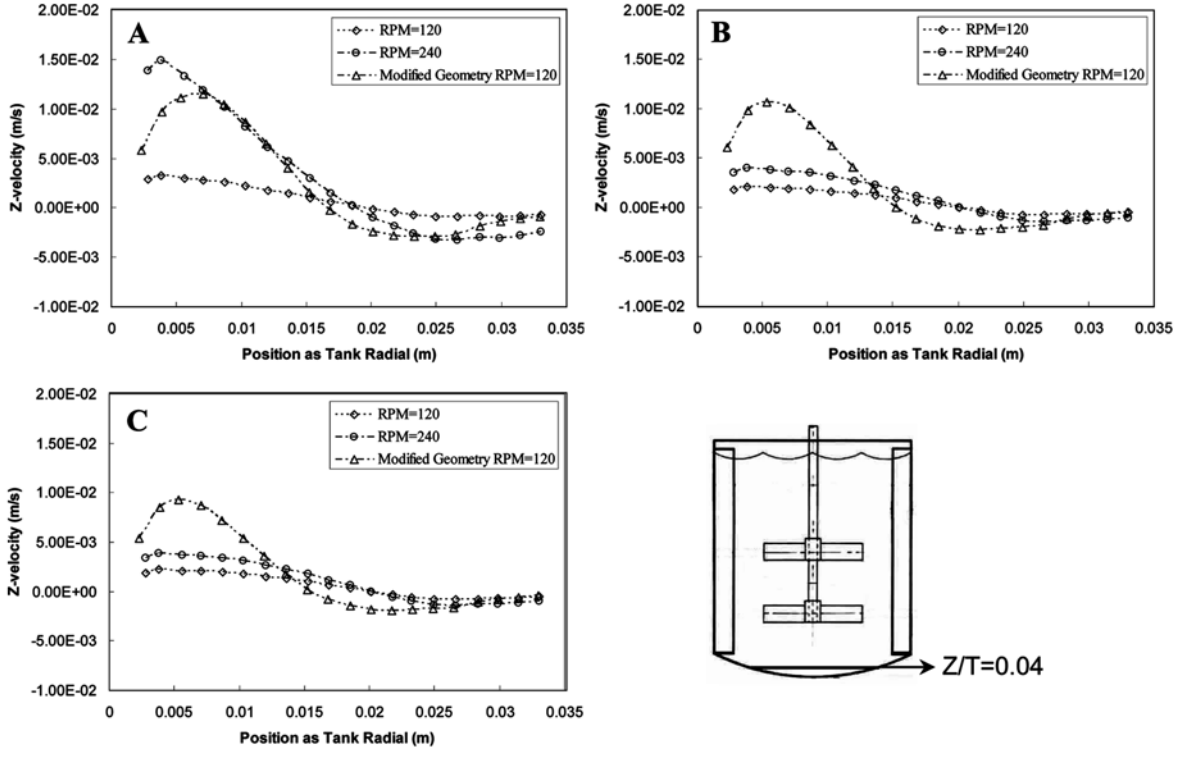

Fig. 7. Profiles of circumferential average axial velocity (m/s) of working volume 2 L bench scale bioreactor at Z/T=0.04. (7A): 10%, (7B): 15%, and (7C): 20% solid concentration. Note: SFF condition: 20 FPU/g of glucan, pH 4.8 to 5.0, *Zymomonas mobilis*, strain 39679 : pZB4L.

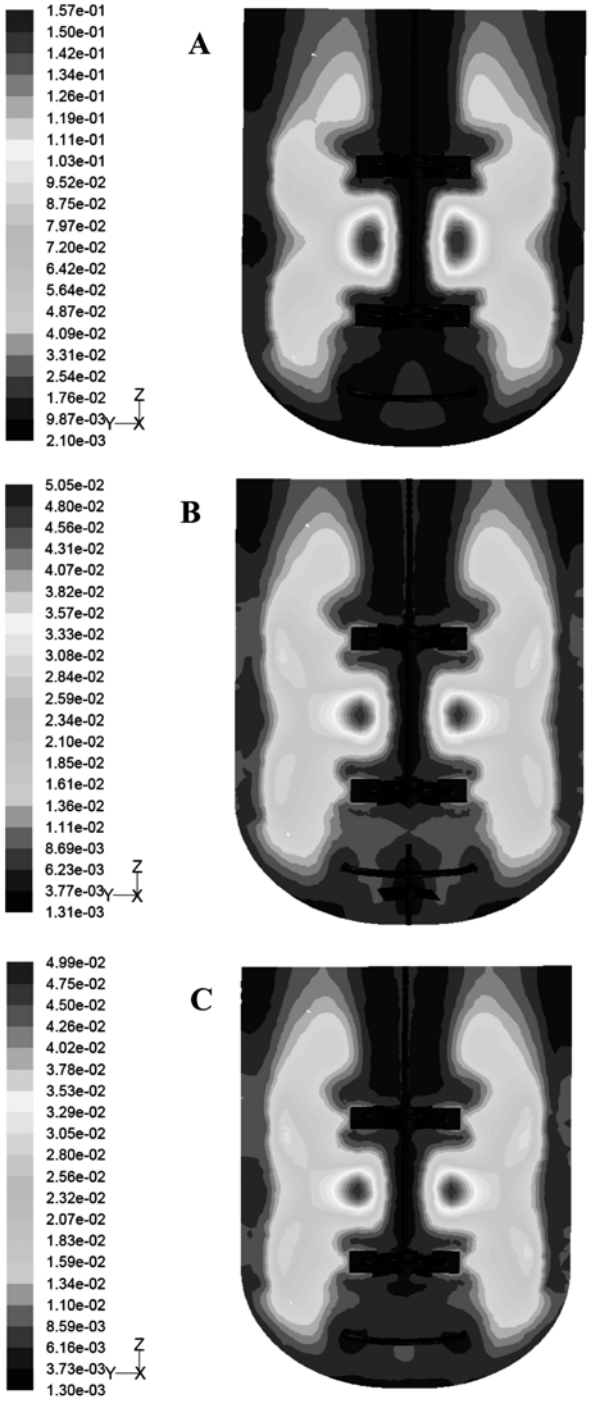

Fig. 8. Distribution of turbulent viscosity (kg/m-s) of working volume 2 L in a bench scale bioreactor. (8A): 200 rpm, (8B): 120 rpm (modified geometry), and (8C): 120 rpm. Note: SFF condition: 15% solid concentration, 20 FPU/g of glucan, pH 4.8 to 5.0, *Zymomonas mobilis*, strain 39679 : pZB4L.

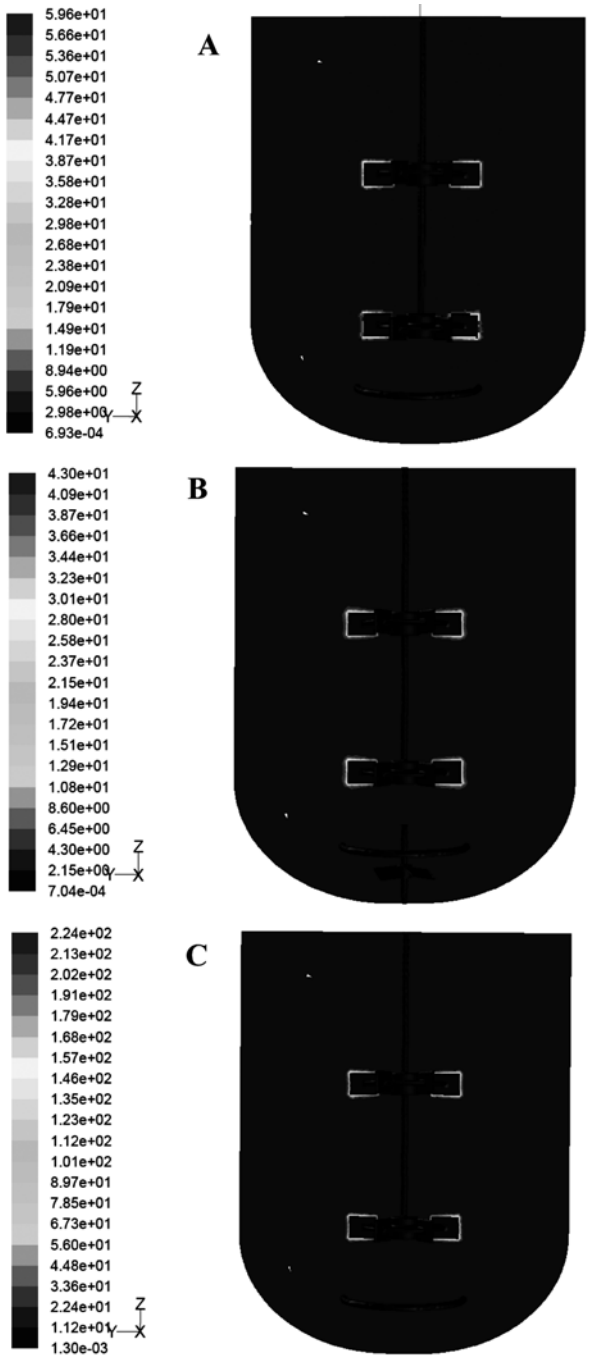

Fig. 9. Distribution of turbulent dissipation rate (ε, m^2/s^3) of working volume 2 L bench scale bioreactor. (9A): 200 rpm, (9B): 120 rpm (modified geometry), and (9C): 120 rpm. Note: SFF condition: 15% solid concentration, 20 FPU/g of glucan, pH 4.8 to 5.0, *Zymomonas mobilis*, strain 39679 : pZB4L.

predicted by the varied viscosity suspension with the maximum values (ε=5.96V_{tip}^3 for 240 RPM, ε=4.30V_{tip}^3 for 120 RPM (modified geometry) ε=2.24V_{tip}^3 for 120 RPM) found in the discharge region and a surrounding zone of relatively high turbulent dissipation rate. The values of ε are close to zero with low dissipation rates elsewhere over all of the operating conditions.

CONCLUSIONS

Flow pattern calculations for potential operating conditions of multiple Rushton six blade agitators in the ellipsoidal bottom tank have been performed to assess mixing behavior. Velocity and shear stress criteria were developed to assess the ability of liquid flow to lift and suspend solids deposited on the bottom surface of the tank. The modeling results will help determine acceptable agitator speeds

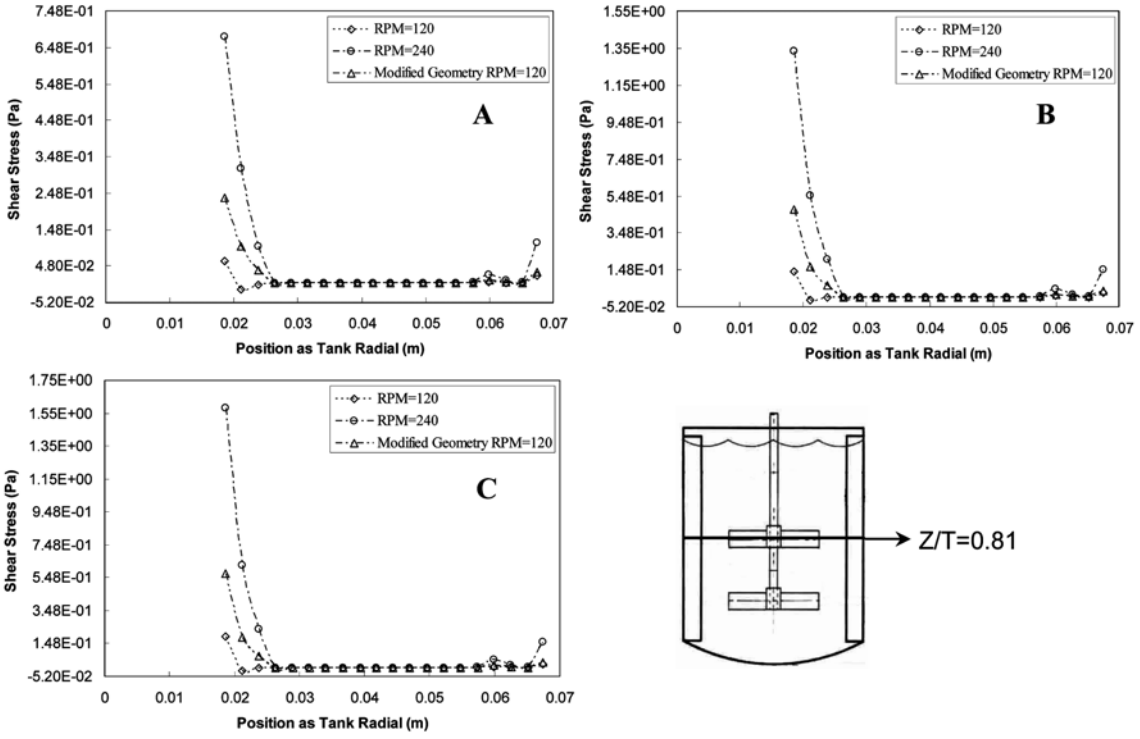

Fig. 10. Shear stress profiles as a function of tank radial position at Z/T=0.81. (10A): 10%, (10B): 15%, and (10C): 20% solid concentration. Note: SFF condition: 20 FPU/g of glucan, pH 4.8 to 5.0, *Zymomonas mobilis*, strain 39679 : pZB4L.

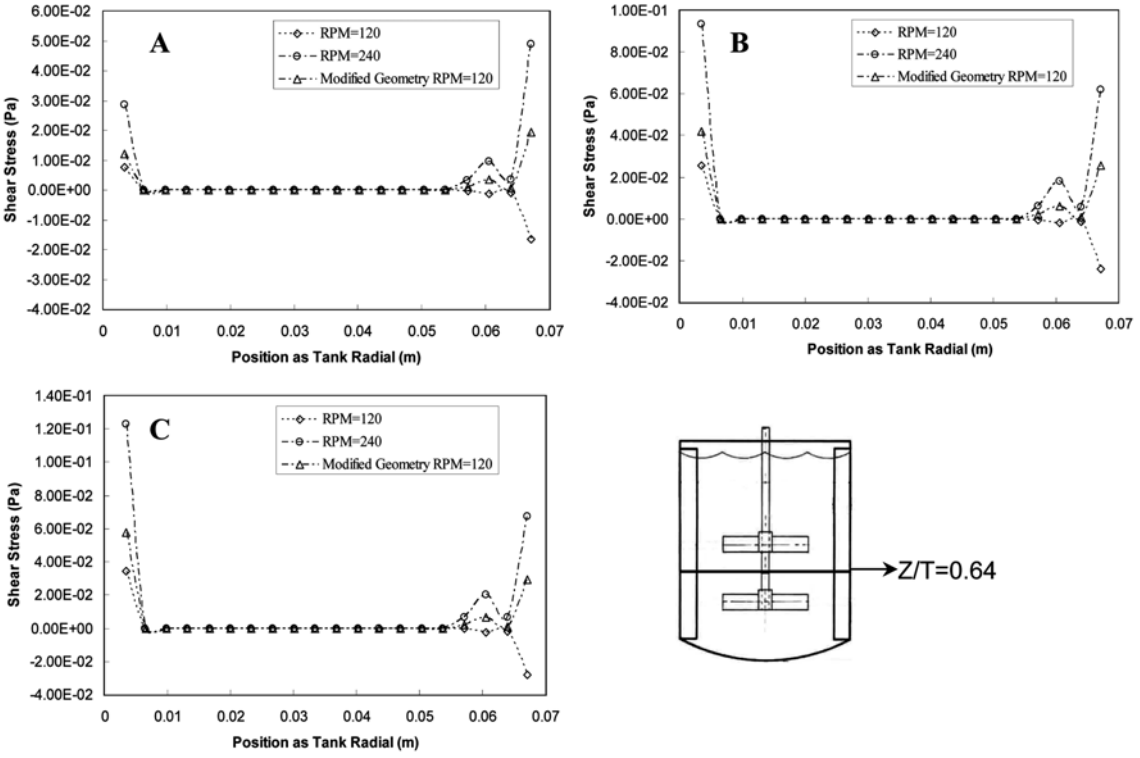

Fig. 11. Shear stress profiles as a function of tank radial position at Z/T=0.64. (11A): 10%, (11B): 15%, and (11C): 20% solid concentration Note: SFF condition: 20 FPU/g of glucan, pH 4.8 to 5.0, *Zymomonas mobilis*, strain 39679 : pZB4L.

and tank liquid levels to ensure suspension of solid particles deposited during high solid fermentation.

A few important observations with regard to the effect of fluid viscosity on fermentation suspension in the laminar flow regime

have been made in this work. The main interest was axial and mixed-flow patterns of the two impellers since they are the most important for viscous suspension mixing. It was found that at various Reynolds numbers, the axial flow component for these impellers was suppressed on the bottom of the tank, such that overall flow was predominantly radial. Specifically, this relatively weak distribution of axial velocities at the bottom of the tank may cause the solid particles to stay around the bottom of the tank. The modified design showed a higher upward axial velocity than original geometry at the tank bottom.

The CFD simulation shows that there is a potential for slow flow or stagnant fluid between the bottom of tank and the fermentor wall and also above the top impeller. In an aerobic fermentation, both of these regions could become depleted of oxygen. High shear rates and energy dissipation rates could be found near both impellers over all operating conditions. Viscosity fields suggest a relationship between primary flow pattern and the location of high viscosity (low mass transfer) regions. These results suggest that correlations for determining the overall heat transfer coefficient in stirred tanks may need to be modified for viscous fluids.

A CFD package such as FLUENT can be used to provide valuable insight into the relationship between fermentor configuration and flow. The results of such studies should prove of interest, especially to engineers who are concerned with bulk mixing, mass transfer and heat transfer in large fermentor with viscous non-Newtonian fluids.

REFERENCES

1. J. Y. Oldshue, *Fluid mixing technology*, McGraw-Hill, New York (1982).
2. R. E. Berson and T. R. Hanley, *Appl. Biochem. Biotechnol*., **124**(3), 935 (2005).
3. G. Montante and F. Magelli, *International J. of CFD*, **19**(3), 253 (2005).
4. A. Mohagheghi, M. Tucker, K. Grohman and C. E. Wyman, *Appl. Biochem. Biotechnol.*, **33**, 67 (1992).
5. D. Spindler, C. E. Wyman, K. Grohman and A. Mohagheghi, *Appl. Biochem. Biotechnol.*, **17**, 279 (1988).
6. E. T. Reese and D. Y. Ryu, *Enzyme and Microbial Technology*, **2**(3), 239 (1980).
7. M. Ursula, R. E. Ali and N. S. John, *Appl. Biochem. Biotechnol*., **98/100**, 463 (2002).
8. FLUENT INC., MIXSIM 2.1 User's Guide, FLUENT INC., Lebanon, NH (2006).
9. FLUENT INC., FLUENT 6 User's Guide, Volume 4, FLUENT INC., Lebanon, NH (2001).